

# A broadly neutralizing human monoclonal antibody is effective against H7N9

Kannan Tharakaraman<sup>a</sup>, Vidya Subramanian<sup>a</sup>, Karthik Viswanathan<sup>b</sup>, Susan Sloan<sup>b</sup>, Hui-Ling Yen<sup>c</sup>, Dale L. Barnard<sup>d</sup>, Y. H. Connie Leung<sup>c</sup>, Kristy J. Szretter<sup>b</sup>, Tyree J. Koch<sup>b</sup>, James C. Delaney<sup>b</sup>, Gregory J. Babcock<sup>b</sup>, Gerald N. Wogan<sup>a,1</sup>, Ram Sasisekharan<sup>a,1</sup>, and Zachary Shriver<sup>b,1</sup>

<sup>a</sup>Department of Biological Engineering, Koch Institute of Integrative Cancer Research, Massachusetts Institute of Technology, Cambridge, MA 02139; <sup>b</sup>Visterra, Inc., Cambridge, MA 02139; <sup>c</sup>School of Public Health, The University of Hong Kong, Hong Kong Special Administrative Region of China, Pokfulam, Hong Kong; and <sup>d</sup>Institute of Antiviral Research, Utah State University, Logan, UT 84322

Contributed by Gerald N. Wogan, February 20, 2015 (sent for review November 20, 2014; reviewed by David J. Topham)

**Emerging strains of influenza represent a significant public health threat with potential pandemic consequences. Of particular concern are the recently emerged H7N9 strains which cause pneumonia with acute respiratory distress syndrome. Estimates are that nearly 80% of hospitalized patients with H7N9 have received intensive care unit support. VIS410, a human antibody, targets a unique conserved epitope on influenza A. We evaluated the efficacy of VIS410 for neutralization of group 2 influenza strains, including H3N2 and H7N9 strains in vitro and in vivo. VIS410, administered at 50 mg/kg, protected DBA mice infected with A/Anhui/2013 (H7N9), resulting in significant survival benefit upon single-dose (–24 h) or double-dose (–12 h, +48 h) administration ( $P < 0.001$ ). A single dose of VIS410 at 50 mg/kg (–12 h) combined with oseltamivir at 50 mg/kg (–12 h, twice daily for 7 d) in C57BL/6 mice infected with A/Shanghai 2/2013 (H7N9) resulted in significant decreased lung viral load ( $P = 0.002$ ) and decreased lung cytokine responses for nine of the 11 cytokines measured. Based on these results, we find that VIS410 may be effective either as monotherapy or combined with antivirals in treating H7N9 disease, as well as disease from other influenza strains.**

antibody | influenza | virus | H7N9

Influenza, a zoonotic viral disease, is responsible for substantial human morbidity and mortality yearly, with periodic elevations due to emergence of novel viral strains, either through mutation or genetic reassortment in a variety of animal reservoirs, including pigs, birds, and seals. Antigenic naivety within the population, coupled with the advent of a virus strain that can effectively transmit via respiratory droplets, can lead to epidemic or pandemic outbreaks. In addition, viruses with increased virulence, such as H5N1 and H7N9, are associated with enhanced morbidity and case fatality, estimated at 30–60% despite the availability of current antiviral therapy.

Patients hospitalized with H7N9 infection typically manifest a high fever and cough, hypoxemia, and opacities and/or consolidations on chest radiology, with associated findings including shock, acute kidney injury, and the development of acute respiratory distress syndrome (ARDS). The high mortality associated with H7N9 infection and development of ARDS is similar to what has been reported for H5N1. An associated cytokine storm has been described in both of these patient groups, with proinflammatory cytokines/chemokines documented in plasma and pulmonary lavage samples (1–3). The increased cytokine responses have recently been correlated with increased severity and mortality observed in patients (2–4). Elevated levels of interleukin (IL)-10, IL-6, IL-8, and macrophage inflammatory protein-1 $\beta$  (MIP-1 $\beta$ ) in plasma were found to be predictive of a less favorable or fatal outcome. Furthermore, IL-1 $\beta$ , interferon (IFN)- $\gamma$ , MIP-1 $\alpha$ , and MIP-1 $\beta$  were all significantly elevated in the bronchial lavage samples at a 100- to 1,000-fold increase compared with plasma concentrations, and tumor necrosis factor (TNF)- $\alpha$  was only detected in the lavage samples. Mouse models for H5N1

and H7N9 infection mimic this cytokine response and the lung pathology of ARDS (2). We therefore sought to examine the role of a broadly neutralizing antibody, VIS410, in mitigating this “cytokine storm” in infected mice and lowering lung viral concentrations in this sublethal H7N9 model. Since this agent would likely be used in combination with a neuraminidase inhibitor, we investigated the effect of VIS410 compared to, and in combination with, oseltamivir.

Additionally, the DBA mouse has been found to have much higher susceptibility to influenza infection than either C56BL/6 or BALB/c mice (5, 6). A variety of influenza viruses, including H5N1 and influenza B viruses, have been shown to be lethal to DBA mice without prior adaptation (7, 8). We reasoned that to complement the cytokine measurements in BALB/c mice, a lethal DBA mouse model could be used to examine the effect of VIS410 on mortality, thereby providing an appropriate model of the significant morbidity and mortality associated with H7N9 infection in humans. We therefore additionally evaluated VIS410 in a lethal model of H7N9 disease.

## Results

### Identification, Recombinant Expression, and Characterization of VIS410.

Our goal was to achieve broad-spectrum coverage with an antibody-based approach that could overcome some of the historical

### Significance

**Emerging influenza subtypes, such as the recently identified H7N9 strains, are of considerable public health concern. Although vaccines are an important countermeasure, influenza vaccines tend to be subtype- and strain-specific, such that they may not be widely available in the event of the human adaptation and spread of an unanticipated strain or subtype. Additionally, influenza strains have demonstrated the ability to develop resistance to existing antivirals, including oseltamivir. As such, there is a need for novel interventions that can treat and/or prevent serious influenza infection. We demonstrate that VIS410, a human mAb, neutralizes a wide range of influenza A viruses and effectively manages H7N9 infection.**

Author contributions: K.T., V.S., K.V., H.-L.Y., Y.H.C.L., K.J.S., T.J.K., J.C.D., G.J.B., G.N.W., R.S., and Z.S. designed research; K.T., V.S., K.V., S.S., H.-L.Y., D.L.B., K.J.S., T.J.K., J.C.D., and G.J.B. performed research; K.T. contributed new reagents/analytic tools; G.N.W., R.S., and Z.S. analyzed data; and G.N.W., R.S., and Z.S. wrote the paper.

Reviewers included: D.J.T., University of Rochester School of Medicine and Dentistry.

Conflict of interest statement: K.V., S.S., K.J.S., T.J.K., J.C.D., G.J.B., and Z.S. are employees of Visterra, Inc. and own equity. R.S. is a shareholder and member of the board of Visterra, Inc.

Freely available online through the PNAS open access option.

<sup>1</sup>To whom correspondence may be addressed. Email: wogan@mit.edu, rams@mit.edu, or zshriver@visterrainc.com.

This article contains supporting information online at [www.pnas.org/lookup/suppl/doi:10.1073/pnas.1502374112/-DCSupplemental](http://www.pnas.org/lookup/suppl/doi:10.1073/pnas.1502374112/-DCSupplemental).

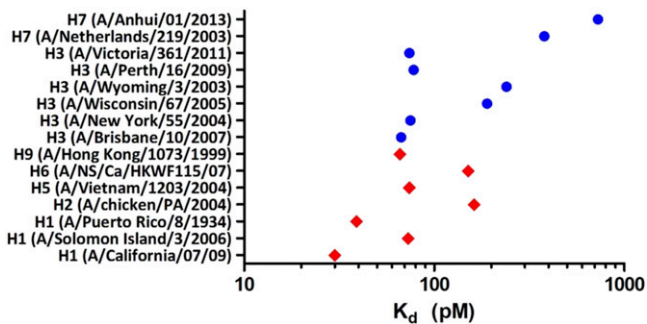


**Fig. 1.** Biochemical characterization of VIS410 binding to influenza HA. VIS410 binding affinity ( $K_d$ , apparent) to a panel of group 1 (red diamonds) and group 2 (blue circles) influenza A HA samples as determined by ELISA, covering the major subtypes that have been known to infect humans.

challenges associated with deployment of such approaches, such as limited spectrum of coverage and/or potency.

To target influenza hemagglutinin (HA), we attempted to engineer an antibody using available structural information on antibody–antigen interfaces. For this effort, we sought to identify an antibody targeting amino acids within the trimeric interface within the stem region of HA, which are highly networked, and therefore potentially limited in their ability to mutate (9). Using a database of nonredundant combinations of complementary determining region (CDR) canonical structures (antibody scaffolds), we selected multiple antibody templates satisfying shape complementarity criteria and systematically engineered energetically favorable, hotspot-like interactions between CDR residues and these anchor residues on HA. The engineering constructs from the multiple templates were evaluated first through *in silico* methods and subsequently through experimentation to test their ability to bind to one or more HAs from group 1 and group 2 (SI Text, Table S1, and Fig. S1). The data from each engineering iteration were used for the subsequent design cycle. VIS410 was selected after multiple rounds of this effort based on its breadth of binding and physicochemical properties, including stability and expression levels. VIS410 is biophysically stable, with a thermal melting transition temperature of  $\sim 70^\circ\text{C}$ , consistent with other commercial antibody products. Analytical analysis of the product indicates that it exists as  $>98\%$  monomer and is stable to aggregation under accelerated conditions ( $37^\circ\text{C}$ ). In addition to inhibiting HA-mediated membrane fusion (Fig. S2), VIS410 exhibits antibody-dependent, cell-mediated cytotoxicity

in *in vitro* assays (Fig. S3), suggesting infected cells can also be targeted for elimination by VIS410.

**Breadth of Binding to Heterosubtypic Influenza Virus HA.** VIS410 was tested for binding to HA from representative group 1 and group 2 subtypes by ELISA. H1, H2, H5, H6, and H9 were chosen as representative HAs from group 1, and H3 and H7 HAs were chosen as group 2 representatives. To account for the high intrasubtypic diversity of H3, a broader panel of H3 HAs was used to assess VIS410 binding. Consistent with targeting a constrained epitope on HA, VIS410 bound all HAs with high avidity (measured apparent  $K_d$ s of 50–730 pM; Fig. 1) as measured by ELISA. To confirm and extend these results, the affinity of VIS410 was measured by surface plasmon resonance on a sparsely HA-coated surface, where binding ( $K_d$ ) was measured in the picomolar to single-digit nanomolar range. *In vitro* VIS410 demonstrated antiviral activity against group 1 and group 2 viruses, indicating that multivalent binding of VIS410 to trimeric HA likely mediates neutralization; this conclusion is supported by previous mechanistic studies conducted for stem-binding antibodies (10, 11) (Table 1). Consistent with its high-affinity binding, VIS410 was found to inhibit viral replication in MDCK cells with  $EC_{50}$ s of  $\sim 0.3$ – $11\ \mu\text{g}/\text{mL}$ , and it was  $10^3$ - to  $10^5$ -fold more potent than ribavirin on a molar basis.

**Therapeutic Administration of VIS410 Rescues Mice Challenged with H3N2 Virus.** As a baseline for studies with H7N9, the prophylactic and therapeutic efficacy of VIS410 was initially evaluated in an H3N2 mouse model, as a representative group 2 strain. Upon intranasal exposure to H3N2, 93% of mock-treated mice succumbed to infection by day 11. VIS410 significantly protected mice against death as measured by total survivors (Fig. 2A;  $P < 0.001$ ), and a single-treatment dose with VIS410 also profoundly affected weight loss (Fig. 2B), as well as timing of death.

VIS410 combination treatment with oseltamivir was also evaluated in an H3N2 sublethal model. The combination of VIS410 at 5 mg/kg (Fig. 2B) plus daily oseltamivir at 10 mg/kg significantly mitigated weight loss compared with either treatment alone from days 5–8 postvirus exposure; this period is the critical time frame in which weight loss is a strong predictor of later mortality due to virus infection. Mitigation in weight loss was also observed for other combinations of VIS410 and oseltamivir. At the highest doses of VIS410 (20 mg/kg) and daily oseltamivir (60 mg/kg), minimal weight loss was observed and the mice returned to their starting weight sooner compared with both placebo and either treatment alone. Thus, taken together, these data demonstrate that VIS410 alone, or in combination with oseltamivir, is efficacious in treating mice infected with a group 2 virus.

**Table 1.** *In vitro* neutralization of group 1 and group 2 influenza A viruses by VIS410

Virus	Inoculum*	VIS410 ( $\mu\text{g}/\text{mL}$ )			Ribavirin ( $\mu\text{g}/\text{mL}$ )			
		$EC_{50}^\dagger$	$CC_{50}^\ddagger$	$SI^\S$	$EC_{50}^\dagger$	$CC_{50}^\ddagger$	$SI^\S$	
H1N1	California 04/2009	300	5.1	$>500$	$>98$	5.4	$>100$	$>195$
H1N1	Solomon Islands	160	1.2	$>500$	$>420$	11	$>100$	$>9.1$
H3N2	Brisbane/10/2007	40	0.3	$>500$	$>1,700$	18	$>100$	$>5.6$
H3N2	Fujian/411/2003	65	0.3	$>500$	$>1,800$	8.7	$>100$	$>12$
H3N2	Panama/2007/99	13	11.0	$>500$	$>45$	8.7	$>100$	$>12$
H3N2	Shangdong/09/93	100	0.6	$>500$	$>890$	3.2	$>100$	$>31$
H3N2	Victoria/3/75	12	4.9	$>500$	$>100$	9.9	$>100$	$>10$
H3N2	Wyoming/03/2003	10	6.8	$>500$	$>74$	22	$>100$	$>4.5$
H5N1	Duck/MN/1525/81	160	1.5	$>500$	$>330$	5.3	$>100$	$>19$

\*Measured as cell culture infective dose ( $CCID_{50}$ ) of virus per well.

$^\dagger$ Measured as 50% toxic concentration ( $CC_{50}$ ) without virus (micrograms per milliliter).

$^\ddagger$ Measured as  $EC_{50}$  (micrograms per milliliter).

$^\S$ Measured as selectivity index ( $SI$ ) =  $CC_{50}/EC_{50}$

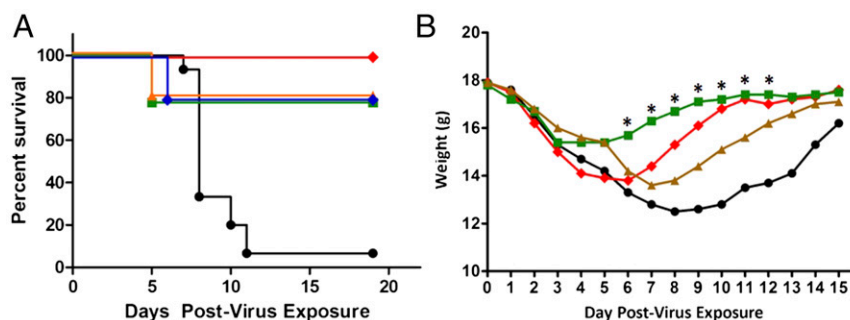


**Fig. 2.** In vivo effect of VIS410 and oseltamivir in a BALB/c mouse model of H3N2. Animals were infected intranasally with a lethal dose of mouse-adapted influenza A/Victoria/3/75 virus (2 LD<sub>50</sub>). Mice were weighed daily to day 15, or until death, and then once again on day 19. (A) Five groups of 10 mice each were administered VIS410 at 2.5 (blue diamonds), 5 (red diamonds), 10 (orange triangles), or 20 (green squares) mg/kg i.p. 48 h after virus exposure; 15 mice received placebo (black circle). Mice were euthanized on the day that 30% weight loss was observed. Statistical inferences were made by two-way ANOVA, followed by pairwise comparisons to compare each treatment group with the placebo group, considering the survival of both (Tukey's multiple comparisons tests). VIS410 had a significant effect on survival ( $P < 0.001$ ). (B) The combination of VIS410 at 5 mg/kg and oseltamivir at 10 mg/kg daily (green squares) had a greater effect on preventing weight loss than did 5 mg/kg VIS410 (red diamonds) or oseltamivir at 10 mg/kg daily (brown triangles) alone ( $*P < 0.001$ ). The placebo is also shown (black circle).

Given the in vivo data with H3N2, the ability of VIS410 to act as an effective treatment for H7N9 was evaluated. We initially examined the ability of VIS410 to bind to H7N9 HA. Binding was assessed by flow cytometry, as well as by ELISA, and demonstrated specific binding with a measured relative  $K_d$  of 0.73 nM (Fig. S4). In in vitro neutralization assays, VIS410 demonstrated neutralizing activity toward H7N9 at  $\sim 50$   $\mu$ g/mL when virus and antibody were premixed, whereas no significant activity was observed when virus and antibody were added concurrently to target cells.

One reason for ambiguous results with the virus neutralization assays might be the system used to measure neutralization. In a standard neutralization assay, a small number of initially infected cells could release progeny virus that is amplified by subsequent infection events. Therefore, to assess VIS410 in a more controlled system, we examined the ability of VIS410 to inhibit H7N9 HA-typed pseudovirus. We found that VIS410 strongly inhibited pseudovirus with an IC<sub>50</sub> of 1.2 nM, comparable to the IC<sub>50</sub> observed for H1 (2.4 nM for A/Puerto Rico/08/1934) (Fig. S5).

Confirming and extending these results, we examined the ability of VIS410 to protect DBA mice against a lethal challenge with A/Anhui/1/2013. Notably, DBA mice are more susceptible to influenza infection than traditional mouse models, such as BALB/c, and thus replicate some aspects of severe disease in humans (12). In an attempt to account for the severity of this model, and to provide a reasonable comparison in cohorts receiving oseltamivir, the dose of VIS410 and oseltamivir was increased to 50 mg/kg. Administration of VIS410 either once prophylactically or twice therapeutically resulted in a significant survival advantage for animals infected with H7N9 ( $P < 0.002$ ). Administration of VIS410 before infection and again 48 h after infection demonstrated superior activity to oseltamivir, which was administered twice daily at 50 mg/kg for 8 d (Fig. 3 A and B;  $P = 0.015$ ). Additionally, VIS410 either alone ( $P = 0.013$ ) or in combination with oseltamivir ( $P < 0.001$ ) resulted in a significant survival advantage compared with oseltamivir alone (Fig. 3 C and D). Finally, in a sublethal H7N9 animal model (2) using a distinct strain of H7N9 (A/Shanghai/2/2013), administration of VIS410 resulted in less viral-induced weight loss (Fig. 4) compared with either mock-treated or oseltamivir-treated animals. Furthermore, when VIS410 was administered in conjunction with oseltamivir, viral concentrations were significantly reduced compared to mock treatment or oseltamivir alone (Fig. 5A;  $P = 0.002$  and  $P = 0.004$  respectively).

The sublethal H7N9 animal model replicates aspects of H7N9-induced pathology observed in human infections (2), including

recent reports of hypercytokinemia in severely infected patients, which was associated with poor prognosis (4). An analysis of a panel of cytokines in H7N9-infected mice indicated an elevation in a number of cytokines, including MIP-1 $\alpha$ /MIP-1 $\beta$ , IFN- $\gamma$ , monocyte chemoattractant protein 1/3 (MCP-1/MCP-3), keratinocyte chemoattractant (KC), and IFN- $\gamma$ -induced protein 10 (IP-10), among others (Fig. 5 and Fig. S6). We note that administration of VIS410 is associated with an increase in IFN- $\gamma$ . Elevation of IFN- $\gamma$  has been associated with a significant protective antiviral effect and is likely one of the mechanisms by which VIS410 offers protection (13, 14). Additionally, when VIS410 was coadministered with oseltamivir, mean IFN- $\gamma$ , MIP-1 $\alpha$ , and IP-10 levels were significantly lower compared with mock-treated mice ( $P < 0.05$ ) and KC trended toward significance ( $P < 0.10$ ). Taken together, this data demonstrates that VIS410 plus oseltamivir can reduce viral replication and virus-induced inflammation in the lungs of H7N9-infected mice.

## Discussion

Given the public health and economic impacts of a regional epidemic or pandemic, significant effort has been focused on surveillance of emerging influenza strains and on vaccine development to counter emerging strains. In the context of controlling emerging influenza strains, such as H5N1 and H7N9, there are a number of challenges. First, as was documented in the case of the 2009 H1N1 pandemic, vaccine availability to the public will likely be delayed and limited. Furthermore, vaccination of immunologically naive individuals against a novel subtype likely requires a prime-boost regimen, further delaying onset of protective immunity. These shortcomings of vaccine strategies support that alternative, supplementary approaches should be considered as prophylactic and therapeutic measures.

Antibody administration to prevent viral infections is well established with licensed therapeutic antibodies for RSV, CMV, hepatitis B virus (HBV), varicella zoster virus, rabies, and vaccinia (15, 16). In the case of influenza, there is also clinical experience to support a potential therapeutic role for antibody. A meta-analysis of studies conducted during the 1918 pandemic using blood products strongly supports a benefit for treated patients (17). Overall, the six studies documented a 21% reduced risk of mortality in treatment groups that had received antiserum. Furthermore, a recent study evaluated the use of convalescent plasma in 93 patients with H1N1 2009 influenza in Hong Kong (18). In this prospective, multicenter, case-control study, mortality was significantly lower in the treatment groups that received convalescent plasma combined with standard of care

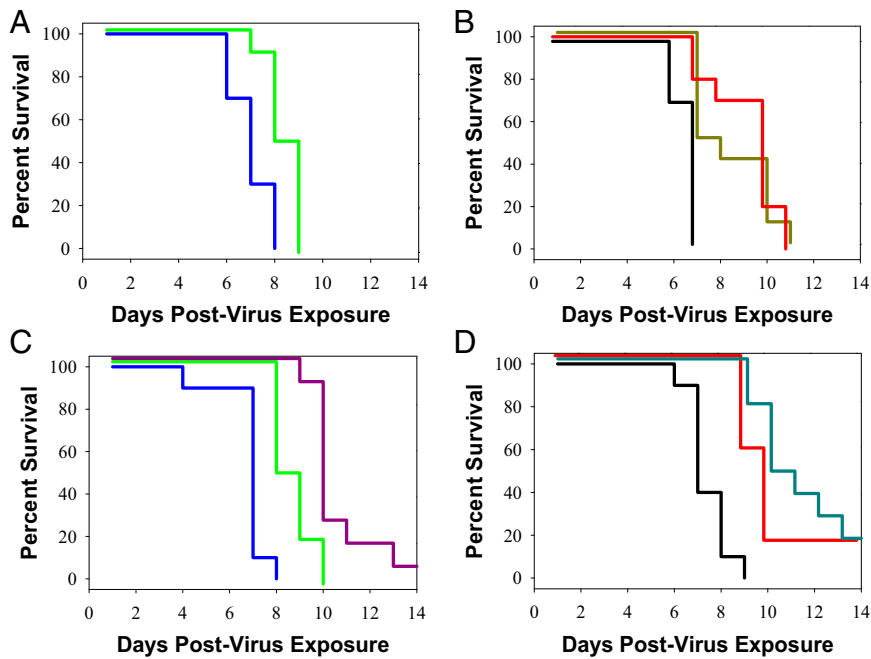


**Fig. 3.** In vivo effect of VIS410 and oseltamivir in a lethal DBA mouse model of H7N9. DBA mice were infected with 1.97 LD<sub>50</sub> of A/Shanghai/2/2013 virus in 25  $\mu$ L of PBS intranasally. (A) Animals treated by oral gavage with oseltamivir, 50 mg/kg daily (green line), had delayed death compared with animals administered water (blue line). (B) VIS410 administered at a dose of 50 mg/kg either once (gold line) or twice (red line) resulted in significantly delayed death compared with PBS-treated animals (black line). (C) Animals treated with a single injection of VIS410 plus daily administration of oseltamivir (purple line) had a significant survival advantage compared with placebo-treated animals (blue line) or animals treated only with oseltamivir (green line). (D) Addition of oseltamivir to two doses of VIS410 (cyan line) resulted in increased survival compared with VIS410 alone (red line) or PBS-treated animals (black line).

compared with the controls who received only standard of care. These data support the potential for a mAb for use as treatment combined with oseltamivir or zanamivir for severe influenza A.

Given the diversity of the influenza virus, particularly in the HA gene, development of a neutralizing mAb that could provide a therapeutic adjunct for diverse strains that are both known and yet to emerge has been a daunting task. Recently, there has been a concerted effort to identify and characterize antibodies that bind to a number of influenza subtypes (so-called “broadly” neutralizing antibodies). Such antibodies have been identified through panning the B-cell repertoire of vaccinated or infected individuals (19, 20), and are infrequent, estimated to be ~0.001–0.01% of the total antibody response (19). To supplement and expand anti-infective antibody discovery, recent developments in computational modeling and structural understanding of antibody–antigen engagement have enabled engineering human and humanized antibodies to increase the breadth of their binding, as well as increase their potency. Several recent examples have demonstrated the possibilities of this approach. In the case of anti-HIV antibodies that target the CD4-binding site, structure-based design of a single mutant, Gly54→Phe, resulted in a 10-fold enhancement in activity (21); additional changes resulted in decreasing possible pathways for resistance development (22, 23). Also, a recent study examined an antidengue antibody and engineered it to increase its affinity to serotype 4 resulting in increased potency to this serotype (24). Notably, this last study was completed in the absence of structural information and utilized an informatics-based approach, using existing information about antibody–antigen engagement. Taken together, these examples and others demonstrate the promise inherent in using engineering approaches to obtain optimized antibody candidates.

In the present study, we demonstrate that an engineered mAb, VIS410, can neutralize divergent group 1 and group 2 strains, including H1N1, H3N2, and H7N9. We show here that VIS410,

alone or in combination with oseltamivir, can mitigate severe H7N9 infection. Finally, through its potent antiviral activity, VIS410 demonstrates the ability to protect against secondary bacterial infection in the mouse model, a common complication reported for influenza-infected patients, including those patients with H7N9 virus (1) (Fig. S7).

Combination of different classes of molecules to control viral replication more effectively and reduce resistance emergence has proven to be a successful strategy for viral diseases, including HCV and HIV. In fact, specifically combining antibody with other antivirals has proved effective for preventing CMV and

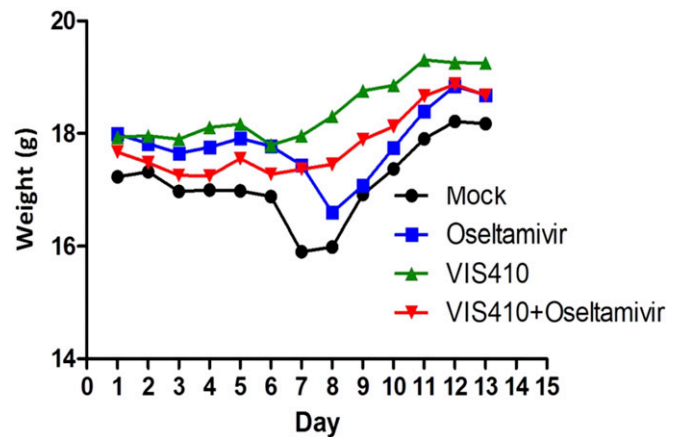


**Fig. 4.** VIS410 protects against effects of H7N9 in a sublethal mouse model of H7N9. C57BL/6 mice were administered vehicle, oseltamivir, VIS410, or VIS410 plus oseltamivir before intranasal inoculation of A/Shanghai/2/2013 virus. Beginning at day 1 postinfection, weight loss was monitored for 12 consecutive days. Results are expressed as mean weight ( $n = 3$ ).

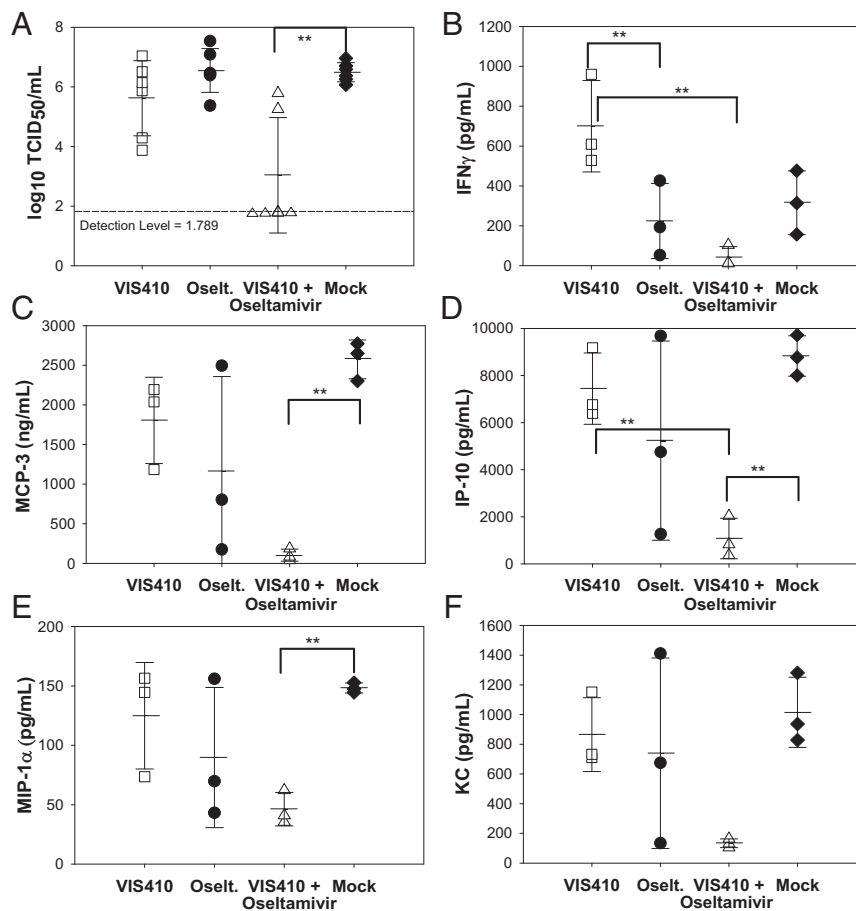


**Fig. 5.** Analysis of virus and cytokine levels in mice administered H7N9. Therapy was initiated 12 h before infection as described in *Materials and Methods*. Animals were administered a sublethal dose of H7N9 and then monitored on day 5 for viral levels (A) and cytokines, including IFN- $\gamma$  (B), MCP-3 (C), IP-10 (D), MIP-1 $\alpha$  (E), and KC (F). Three animals were used per cohort, except for determination of viral titers ( $n = 6$ ), and were mock-treated ( $\blacklozenge$ ), VIS410-treated ( $\square$ ), oseltamivir-treated ( $\bullet$ ), or cotreated with both oseltamivir and VIS410 ( $\Delta$ ). Tukey posttest analysis identified the groups that were significantly different from one another (\*\* $P < 0.05$ ). Differences in IFN- $\gamma$ , MCP-3, IP-10, and MIP-1 $\alpha$  were significant, whereas the difference for KC trended toward significance ( $P < 0.1$ ).

HBV infections. For influenza, it is clear that dual deployment of neuraminidase inhibitors is problematic from the standpoint of a shared mechanism of action, the potential for shared cross-resistance, and potential antagonism of antiviral activity (25). Furthermore, resistance development to oseltamivir and the adamantanes is widespread in H1N1 and has been already reported for H7N9, without having an impact on virus fitness (26). Therefore, development of a broadly neutralizing human mAb, such as VIS410, could provide an important addition to countermeasures for severe influenza, including H7N9, either alone or combined with other antiviral drugs.

## Materials and Methods

**Recombinant Expression of VIS410 Antibody.** Initial recombinant expression of antibody was carried out in HEK-293F FreeStyle suspension cells (Invitrogen) using recommended conditions. Cells were transfected with Poly-ethyleneimine Max (PEI-MAX; PolySciences) with equivalent amounts of heavy-chain- and light-chain-containing plasmids. Seven days posttransfection, cells were harvested by centrifugation and supernatants were sterile-filtered. Antibody was purified using Protein A resin (Pierce), buffer-exchanged with PBS, and concentrated as required. In lieu of transfection, later studies used a stable CHO cell line for the production of VIS410, and purification was performed as described above.

**ELISA Binding Assays.** Recombinant HA (Protein Sciences Corporation) was coated on 96-well microtiter plates (Immuno Maxisorp; Nunc) and blocked with 5% (wt/vol) Blotto (Santa Cruz Biotechnology) in 1 $\times$  PBS. Serially diluted

antibody was added, and binding was detected using HRP-conjugated goat antihuman IgG (Fc-specific; Bethyl Laboratories), followed by development with 3,3',5,5'-Tetramethylbenzidine solution (KPL). The absorbance at 450 nm was measured using a Spectramax plate reader (Molecular Devices), and data were analyzed with the Softmax software (Molecular Devices).

**Pseudovirus Infection Assay.** Codon-optimized HA genes were synthesized (DNA2.0) and cloned into pLPVSV-G (Invitrogen), replacing the VSV-G gene with the influenza HA gene. Pseudotyped lentivirus was generated by transient transfection of HEK-293T/17 cells with the pLP-HA and an HIV-1 backbone that contained a deletion to prevent envelope glycoprotein expression and an inserted luciferase gene (pNL Luc AM). Transfection medium consisted of Dulbecco's Modified Eagle Medium (DMEM) supplemented with 10% FBS. Twenty-four hours following transfection, the medium was replaced with DMEM/3% FBS containing 50 mU/mL neuraminidase purified from *Vibrio cholerae* (Sigma). Transfectants were incubated for an additional 48 h, and the medium was harvested, treated with 10  $\mu$ g/mL TPCK-trypsin (Sigma) for 1 h at 37  $^{\circ}$ C, and frozen at  $-80^{\circ}$  C. A fixed volume of pseudovirus-containing supernatants that yielded  $\sim 300,000$  relative light units was incubated with varying concentrations of antibody for 1 h at 37  $^{\circ}$ C. Antibody/pseudovirus mixtures were applied to  $2 \times 10^4$  HEK-293T/17 or MDCK cells in 96-well tissue culture plates and incubated for 72 h at 37  $^{\circ}$ C. One-Glo luciferase reagent (Promega) was added to each well and incubated for 4 min at room temperature. Light output was measured using a BioTek Synergy 2 luminometer.

**Murine Lethal Challenge Model.** Studies with H3N2 (A/Victoria/3/75) and H7N9 (A/Anhui/1/2013) viruses were performed at the Institute of Antiviral Research

at Utah State University. The animal experiments were conducted with the approval of the Institutional Animal Care and Use Committee of Utah State University in the American Association for the Accreditation of Laboratory Animal Care-accredited Laboratory Animal Research Center in accordance with the NIH *Guide for the Care and Use of Laboratory Animals* (27). Eight- to ten-week-old female DBA or BALB/c mice were obtained from Charles River Laboratories for the H7N9 (A/Anhui/1/2013) and H3N2 (A/Victoria/3/1975) experiments, respectively. Mice were maintained on Wayne Lab Blox and tap water ad libitum and quarantined for 24 h before use. Influenza A/Anhui/1/2013 (H7N9) virus was obtained from the CDC. A virus pool was prepared in MDCK cells and pretitrated in young adult DBA mice before its use. Mice were infected intranasally with concentrations of virus equal to one LD<sub>100</sub> of A/Anhui/1/2013 or 2 LD<sub>50</sub> of A/Victoria/3/1975. In all experiments, one group of 10 mice was administered VIS410 antibody i.p. at 2.5–50 mg/kg 24 h before virus exposure, 48 h after virus exposure, or both. An additional 10 mice received oral oseltamivir at 50 mg/kg twice daily for 8 d, beginning 24 h before virus exposure. Placebo groups receiving mock administration either i.p. or orally were also used. Mice were weighed daily up to day 13, or until death, beginning just before virus exposure. Adverse events for which observations were made included ruffling of fur, lethargy, paralysis, incontinence, repetitive circular motion, and aggression. Survival analyses were completed using the Kaplan–Meier graphing method, and pairwise comparisons of survivor curves (placebo vs. any treatment) were analyzed by the Mantel–Cox log rank test.

**Sublethal Challenge Model.** Studies with H7N9 (A/Shanghai/2/2013) in the C57BL/6 mouse model were conducted at the biosafety level-3 facility at the Li Ka Shing Faculty of Medicine, the University of Hong Kong, under approved guidelines and ethics. Stock virus titer was determined to be  $6 \times 10^6$  pfu/mL. Groups of 14 C57BL/6 mice obtained from the Laboratory Animal

Unit at The University of Hong Kong were inoculated with 1,500 plaque-forming units (1.97 LD<sub>50</sub>) of A/Shanghai/2/2013 virus in 25  $\mu$ L of PBS intranasally. Four different regimens were used starting 12 h before infection: (i) mock treatment using PBS via i.p. injection, (ii) a single dose of VIS410 at 50 mg/kg via i.p. injection, (iii) oseltamivir phosphate via oral gavage at 40 mg/kg twice daily for 7 d, or (iv) a single dose of VIS410 (50 mg/kg, i.p. injection) and oseltamivir phosphate via oral gavage at 40 mg/kg twice daily for 7 d. At day 5 postinoculation, six mice per group were killed and lung tissue was harvested to determine virus titers ( $n = 6$  for each) and cytokine levels ( $n = 3$  for each). For virus titration, mouse lungs were homogenized in 1 mL of PBS and titrated in MDCK cells to determine viral titers (log<sub>10</sub> TCID<sub>50</sub> per milliliter). For cytokine measurements, mouse lungs were homogenized in 1 mL of PBS and supernatant was clarified by centrifugation. Levels of cytokines were determined using FlowCytomix (eBioscience). Statistical comparisons of cytokine levels were made first using one-way ANOVA, followed by the Turkey posttest. Additional analysis using the nonparametric Kruskal–Wallis test was used to confirm this analysis.

**ACKNOWLEDGMENTS.** We thank Ka-Tim Choy, Candy Chuk Kwan Ho, Ooiean Teng, and Sin Fun Sia at the University of Hong Kong for excellent technical assistance. We also thank Andrew Wollacott for his assistance with sequence and structural analysis and Hedy Adari and April Blodgett for their assistance with VIS410 characterization. This work was funded in part by an NIH Merit Award (R37 GM057073-13 to R.S.), and the National Research Foundation supported Interdisciplinary Research group in Infectious Diseases of SMART (Singapore MIT alliance for Research and Technology). In vitro and in vivo assessment of VIS410 was completed, in part, through the Preclinical Services for Researchers Program of the Division of Microbiology and Infectious Diseases of the National Institute of Allergy and Infectious Diseases (Contract HHSN2722010000391).

- Wang XF, et al. (2013) Clinical features of three avian influenza H7N9 virus-infected patients in Shanghai. *Clin Respir J* 8(4):410–416.
- Mok CK, et al. (2013) Pathogenicity of the novel A/H7N9 influenza virus in mice. *MBio* 4(4):e00362–13.
- Gao HN, et al. (2013) Clinical findings in 111 cases of influenza A (H7N9) virus infection. *N Engl J Med* 368(24):2277–2285.
- Wang Z, et al. (2014) Early hypercytokinemia is associated with interferon-induced transmembrane protein-3 dysfunction and predictive of fatal H7N9 infection. *Proc Natl Acad Sci USA* 111(2):769–774.
- Kim JI, et al. (2013) DBA/2 mouse as an animal model for anti-influenza drug efficacy evaluation. *J Microbiol* 51(6):866–871.
- Boon AC, et al. (2009) Host genetic variation affects resistance to infection with a highly pathogenic H5N1 influenza A virus in mice. *J Virol* 83(20):10417–10426.
- Boon AC, et al. (2010) Cross-reactive neutralizing antibodies directed against pandemic H1N1 2009 virus are protective in a highly sensitive DBA/2 mouse influenza model. *J Virol* 84(15):7662–7667.
- Pica N, et al. (2011) The DBA.2 mouse is susceptible to disease following infection with a broad, but limited, range of influenza A and B viruses. *J Virol* 85(23):12825–12829.
- Soundararajan V, et al. (2011) Networks link antigenic and receptor-binding sites of influenza hemagglutinin: Mechanistic insight into fitter strain propagation. *Sci Rep* 1:200.
- Messer WB, et al. (2014) Dengue virus envelope protein domain III hinge determines long-lived serotype-specific dengue immunity. *Proc Natl Acad Sci USA* 111(5):1939–1944.
- Brandenburg B, et al. (2013) Mechanisms of hemagglutinin targeted influenza virus neutralization. *PLoS One* 8(12):e80034.
- Bouvier NM, Lowen AC (2010) Animal Models for Influenza Virus Pathogenesis and Transmission. *Viruses* 2(8):1530–1563.
- Paolini R, Bernardini G, Molfetta R, Santoni A (2015) NK cells and interferons. *Cytokine Growth Factor Rev* 26(2):113–120.
- Price GE, Gaszewska-Mastarlarz A, Moskophidis D (2000) The role of alpha/beta and gamma interferons in development of immunity to influenza A virus in mice. *J Virol* 74(9):3996–4003.
- Casadevall A, Dadachova E, Pirofski LA (2004) Passive antibody therapy for infectious diseases. *Nat Rev Microbiol* 2(9):695–703.
- ter Meulen J (2007) Monoclonal antibodies for prophylaxis and therapy of infectious diseases. *Expert Opin Emerg Drugs* 12(4):525–540.
- Luke TC, Kilbane EM, Jackson JL, Hoffman SL (2006) Meta-analysis: Convalescent blood products for Spanish influenza pneumonia: A future H5N1 treatment? *Ann Intern Med* 145(8):599–609.
- Hung IF, et al. (2011) Convalescent plasma treatment reduced mortality in patients with severe pandemic influenza A (H1N1) 2009 virus infection. *Clin Infect Dis* 52(4):447–456.
- Hashem AM, et al. (2010) Universal antibodies against the highly conserved influenza fusion peptide cross-neutralize several subtypes of influenza A virus. *Biochem Biophys Res Commun* 403(2):247–251.
- Ekiert DC, et al. (2011) A highly conserved neutralizing epitope on group 2 influenza A viruses. *Science* 333(6044):843–850.
- Diskin R, et al. (2011) Increasing the potency and breadth of an HIV antibody by using structure-based rational design. *Science* 334(6060):1289–1293.
- Diskin R, et al. (2013) Restricting HIV-1 pathways for escape using rationally designed anti-HIV-1 antibodies. *J Exp Med* 210(6):1235–1249.
- Sethi A, Tian J, Derdeyn CA, Korber B, Gnanakaran S (2013) A mechanistic understanding of allosteric immune escape pathways in the HIV-1 envelope glycoprotein. *PLoS Comput Biol* 9(5):e1003046.
- Tharakaraman K, et al. (2013) Redesign of a cross-reactive antibody to dengue virus with broad-spectrum activity and increased in vivo potency. *Proc Natl Acad Sci USA* 110(17):E1555–E1564.
- Duval X, et al.; Bivir Study Group (2010) Efficacy of oseltamivir-zanamivir combination compared to each monotherapy for seasonal influenza: A randomized placebo-controlled trial. *PLoS Med* 7(11):e1000362.
- Hai R, et al. (2013) Influenza A(H7N9) virus gains neuraminidase inhibitor resistance without loss of in vivo virulence or transmissibility. *Nat Commun* 4:2854.
- Committee on Care and Use of Laboratory Animals (1996) *Guide for the Care and Use of Laboratory Animals* (Natl Inst Health, Bethesda), DHHS Publ. No. (NIH) 85-23.
- McCullers JA (2004) Effect of antiviral treatment on the outcome of secondary bacterial pneumonia after influenza. *J Infect Dis* 190(3):519–526.
- Soundararajan V, et al. (2011) Networks link antigenic and receptor-binding sites of influenza hemagglutinin: Mechanistic insight into fitter strain propagation. *Scientific Reports* 1:200.
- Thyagarajan B, Bloom JD (2014) The inherent mutational tolerance and antigenic evolvability of influenza hemagglutinin. *eLife* 3:e03300.